Cancer Cell
Article

TNFR1 Signaling and IFN-γ Signaling Determine whether T Cells Induce Tumor Dormancy or Promote Multistage Carcinogenesis

Nele Müller-Hermelink,[1,10] Heidi Braumüller,[1,10] Bernd Pichler,[2,10] Thomas Wieder,[1] Reinhard Mailhammer,[3] Katrin Schaak,[1] Kamran Ghoreschi,[1] Amir Yazdi,[1] Roland Haubner,[4,5] Christian A. Sander,[6] Ralph Mocikat,[7] Markus Schwaiger,[4] Irmgard Förster,[8] Ralph Huss,[9] Wolfgang A. Weber,[4] Manfred Kneilling,[1] and Martin Röcken[1,*]
[1]Department of Dermatology, Eberhard Karls University, Liebermeisterstrasse 25, 72076 Tübingen, Germany
[2]Laboratory for Preclinical Imaging and Imaging Technology of the Werner Siemens-Foundation, Department of Radiology, Eberhard Karls University, Röntgenweg 13, 72076 Tübingen, Germany
[3]Helmholtz Center Munich, German Research Center for Environmental Health, Institute of Clinical Molecular Biology and Tumor Genetics, Marchioninistrasse 25, 81377 Munich, Germany
[4]Department of Nuclear Medicine, University of Freiburg, Hugstetterstrasse 55, 79106 Freiburg, Germany
[5]Department of Nuclear Medicine, Technical University, Ismaningerstrasse 22, 81675 Munich, Germany
[6]Department of Dermatology, AK St. Georg, Lohmuehlenstrasse 5, 20099 Hamburg, Germany
[7]Helmholtz Center Munich, German Research Center for Environmental Health, Institute of Molecular Immunology, Marchioninistrasse 25, 81377 Munich, Germany
[8]Institut für Umweltmedizinische Forschung, Department of Molecular Immunology, Heinrich-Heine-University of Düsseldorf, Auf'm Hennekamp 50, 40225 Düsseldorf, Germany
[9]Institute of Pathology, Ludwig-Maximilians-University, Thalkirchnerstrasse 46, 80337 Munich, Germany
[10]These authors contributed equally to this work
*Correspondence: mrocken@med.uni-tuebingen.de
DOI 10.1016/j.ccr.2008.04.001

SUMMARY

Immune responses may arrest tumor growth by inducing tumor dormancy. The mechanisms leading to either tumor dormancy or promotion of multistage carcinogenesis by adaptive immunity are poorly characterized. Analyzing T antigen (Tag)-induced multistage carcinogenesis in pancreatic islets, we show that Tag-specific $CD4^+$ T cells home selectively into the tumor microenvironment around the islets, where they either arrest or promote transition of dysplastic islets into islet carcinomas. Through combined TNFR1 signaling and IFN-γ signaling, Tag-specific $CD4^+$ T cells induce antiangiogenic chemokines and prevent $\alpha_v\beta_3$ integrin expression, tumor angiogenesis, tumor cell proliferation, and multistage carcinogenesis, without destroying Tag-expressing islet cells. In the absence of either TNFR1 signaling or IFN-γ signaling, the same T cells paradoxically promote angiogenesis and multistage carcinogenesis. Thus, tumor-specific T cells can directly survey multistage carcinogenesis through cytokine signaling.

INTRODUCTION

Malignant tumors evolve along multistage programs that require establishment of a tumor stroma, neoangiogenesis, and reprogramming of cell metabolism, leading to the expression of tumor-associated antigens (TAA) (Bissell and Radisky, 2001; Boon et al., 2006; Folkman et al., 1989; Hanahan and Weinberg, 2000). This program is influenced by innate immune cells that promote aberrant growth of the $\alpha_v\beta_3$ integrin-expressing vessels, required for the transition of premalignant dysplasias into

SIGNIFICANCE

Previous studies revealed that $CD4^+$ T cells reject transplanted tumors better than cytotoxic $CD8^+$ T cells, but the effects of $CD4^+$ T cells on multistage carcinogenesis remain enigmatic. Studying the effects of tumor-specific, IFN-γ-producing $CD4^+$ T cells on T antigen-driven multistage carcinogenesis, we found that T cells can either arrest or promote multistage carcinogenesis through cytokine signaling. Arresting multistage carcinogenesis strictly requires concerted IFN-γ signaling and TNFR1 signaling; if either signaling is impaired, the same T cells significantly promote angiogenesis and multistage carcinogenesis. The data show that tumor-specific T cells can directly affect multistage carcinogenesis and characterize the tightly regulated cytokine interactions that determine whether a specific T cell response arrests or accelerates progression from premalignant dysplasia into cancer.

carcinomas and further cancer progression (Arnott et al., 2004; Bergers et al., 2000; Bhowmick et al., 2004; de Visser et al., 2006; Lin et al., 2001; Moore et al., 1999; Nozawa et al., 2006; Soucek et al., 2007; Suganuma et al., 1999).

Adaptive immune responses against TAA may also influence carcinogenesis. T and B cell (*RAG*$^{-/-}$)- or interferon γ receptor (*IFN-γR*$^{-/-}$)- deficient mice have a 10-fold increase in infection-associated malignancies, but not of other malignancies (Shankaran et al., 2001; Street et al., 2002). T cells and IFN-γ may arrest certain established tumors in mice and probably also in humans (Koebel et al., 2007; MacKie et al., 2003; Sato et al., 2005), and certain vaccine protocols protect mice even against tumors that develop under a strong transgenic tumor promotor (Holmgren et al., 2006; Nanni et al., 2001; Pannellini et al., 2006; Willimsky and Blankenstein, 2005). Yet, the molecular mechanisms underlying the T cell-mediated control of multistage carcinogenesis remain unknown.

Most work focused on cytolytic CD8$^+$ T cells (CTL). But the role of CTL in tumor cell killing under clinical conditions is still not understood, as strong TAA-specific CTL responses don't correlate with effective tumor protection (Nelson et al., 2001; Valmori et al., 2001; Willimsky and Blankenstein, 2005; Yee et al., 2002). Even though CTL can eradicate freshly transplanted tumor cells, numerous data suggest that IFN-γ-producing CD4$^+$ T cells (Th1) prevent growth and development of transplanted tumors more efficiently than CTL. As CD4$^+$ T cells cannot recognize major histocompatibility complex (MHC) class II-negative tumor cells, Th1 cells may provide bystander help for CTL, induce cytotoxic macrophages, affect tumor cell differentiation or tumor stroma, or inhibit vessel formation (Chamoto et al., 2006; Daniel et al., 2005; Ganss et al., 2002; Greenberg, 1991; Mocikat et al., 2003; Mumberg et al., 1999; Nishikawa et al., 2005; Qin and Blankenstein, 2000; Rosenberg et al., 2004).

Most insights into tumor immunology result from transplanted monoclonal tumors that do not follow the events of multistage carcinogenesis. To investigate the effects of TAA-specific CD4$^+$ T cells on endogenous, multistage carcinogenesis, we analyzed mice that express T antigen (Tag) under the control of the rat insulin promoter (RIP1-Tag2). Tag inhibits the tumor suppressors p53 and retinoblastoma protein (Rb) (Casanovas et al., 2005a). RIP1-Tag2 mice develop islet adenomas with new $\alpha_v\beta_3$ integrin-expressing blood vessels of abnormal configuration in 20% of the islets. Within 6 weeks, two to five of those adenomas progress into carcinomas (Bergers et al., 1999; Casanovas et al., 2005b).

Here we show that Tag-specific CD4$^+$ T cells expressing a T cell receptor (TCR) specific for Tag peptide 362-384 (TCR2; Forster et al., 1995) directly regulate multistage carcinogenesis through cytokine signals. Tag-specific Th1 cells induced a state of tumor dormancy. Paradoxically, in the absence of either IFN-γ signaling or tumor necrosis factor p55 receptor (TNFR1) signaling the same Tag-specific Th1 cells strongly promoted multistage carcinogenesis.

RESULTS

Selective Homing of Tag-Specific CD4$^+$ T Cells into the Peritumoral Microenvironment

To study the impact of TAA-specific CD4$^+$ T cells on multistage carcinogenesis in endogenous tumors, we transferred IFN-γ-producing, Tag-specific Th1 cells into RIP1-Tag2 mice that express the Tag oncogene in all islet cells. CD4$^+$ TCR2 cells specific for Tag peptide 362–384 were stimulated in vitro with Tag peptide 362-384, CpG-oligonucleotide 1668, and antigen-presenting cells (APC) to generate Th1 cells. After 1 week, >95% cells expressed the idiotypic TCR2 and produced IFN-γ but no interleukin (IL-) 4 (Figure 1A). They were termed Tag-Th1 cells.

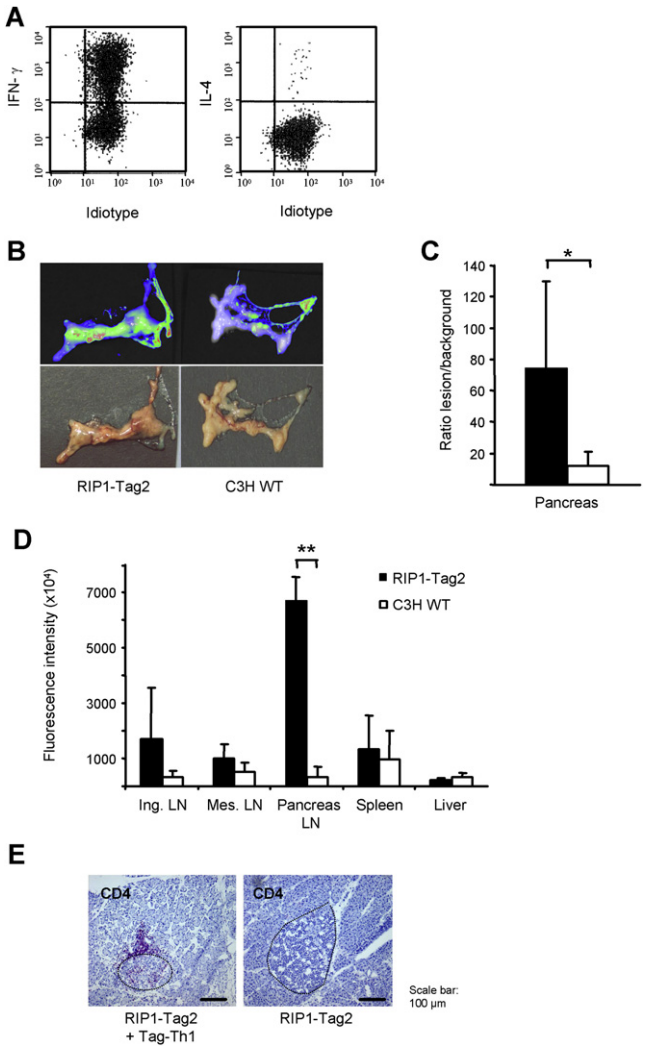

Figure 1. Specific Homing of Tag-Th1 Cells into the Tumor Microenvironment and the Tumor-Draining Lymph Node

(A) Intracytoplasmatic staining of Tag-specific Th1 cells isolated from TCR2 mice. After stimulation with ionomycin/PMA, idiotypic TCR expression and intracellular cytokine load were determined by FACS.

(B) (Top) Fluorescence images of pancreas and omentum 3 days after i.p. injection of Cy5-labeled Tag-Th1 cells into a RIP1-Tag2 (left) or a C3H wild-type mouse (right). Red and green colors indicate increased fluorescence from Tag-Th1 cells. (Bottom) Corresponding bright field images.

(C) Mean ratio of tumor to normal pancreas (background) fluorescence ± SD (n = 5) of Cy5-labeled Tag-Th1 cells on day three after i.p. injection into RIP1-Tag2 mice (black bar) or C3H wild-type littermates (white bar). *p = 0.04.

(D) Mean fluorescence intensity ± SD (n = 5) of liver, spleen, draining, and distant lymph nodes (LN) from the same experiment as in (C). **p < 0.01.

(E) Immunohistochemistry of CD4$^+$ lymphocytes in the peritumoral microenvironment of Tag-Th1 cell- (left) or sham-treated (right) RIP1-Tag2 mice.

We treated 7- to 8-week-old RIP1-Tag2 mice once weekly with 10^7 Tag-Th1 cells. At this time, about 20% of islets had switched on angiogenesis, characterized by the presence of $\alpha_v\beta_3$-expressing vessels, and transformed into hyper- or dysplastic adenomas, which decreased blood glucose to around 90 mg/dl. These changes precede the transition of dysplastic islets into carcinomas by 2 weeks.

Tag-Th1 cells were labeled with Cy5 fluorescent dye to follow their migration in vivo. Within 3 days, intense fluorescence was detected in the pancreas of RIP1-Tag2 mice but not in that of C3H controls (Figures 1B and 1C). Fluorescent Tag-Th1 cells were also enriched specifically in the pancreas-draining lymph node of RIP1-Tag2 but not in that of nontransgenic C3H mice (Figure 1D). We also detected Tag-Th1 cells in spleen and mesenteric lymph nodes. These Tag-Th1 cells were functional based on Tag-specific proliferation and IFN-γ production. No Tag-reactive Th1 cells appeared in sham-treated RIP1-Tag2 mice (Figure S1 available online).

To localize the Tag-Th1 cells more precisely, we performed autoradiography of labeled Tag-Th1 cells and immune histology. These analyses revealed homing of Tag-Th1 cells around the islets, where they established lymph follicle-like structures (Figure 1E). Infiltration of islets was a rare event.

Tag-Th1 Cells Double Survival Time without Causing Autoimmune Diabetes

We next analyzed the effects of Tag-Th1 cells on blood glucose and survival in 7- to 8-week-old mice with established adenomas. Starting from the day of treatment, sham-treated mice lived 8 weeks, while Tag-Th1 treated mice lived up to 16 weeks, which equals a doubling of the survival time (Figure 2A). Irradiation alone did not affect survival of RIP1-Tag2 mice (Figure S2). In RIP1-Tag2 mice, a similar prolongation of life was previously obtained by treating these mice with in vitro activated, islet cell-specific CTL that destroyed all insulin-producing cells and caused severe diabetes (Speiser et al., 1997). In contrast, treatment with Tag-Th1 cells did not cause diabetes in RIP1-Tag2 mice from >10 independent experiments. The mice had slightly subnormal but stable blood glucose levels (Figure 2B; $p < 0.0005$). Thus, transfer of "auto"-reactive Tag-Th1 cells did not destroy the Tag-expressing islet cells, as 100% of the cells express Tag.

We also started treatment with Tag-Th1 cells at earlier stages of malignant transformation, i.e., at 5 weeks of age, when the earliest signs of tumor angiogenesis and dysplasia appear. Under these conditions, Tag-Th1 cells even doubled the total life span, as half of the mice lived beyond week 30 (Figure 2C). Again, none of the mice developed diabetes.

Tag-Th1 Cells Arrest Tumor Growth and Tumor Angiogenesis

To confirm that Tag-Th1 cells arrested tumor growth without destroying islet cells, we first performed pancreas histology from 12-week-old C3H, untreated RIP1-Tag2 or RIP1-Tag2 mice treated for 6 weeks with Tag-Th1 cells. The pancreas of C3H mice harbors small islets (Figure 3A). RIP1-Tag2 mice had two to three carcinomas with large vascular spaces, the mature ones surrounded by α-actin-expressing pericytes (Figure 3B). X-ray treatment alone (2 Gy) did not influence carcinoma development (Figure 3C). Following treatment with Tag-Th1 cells, tumors seemed to be arrested at the level of premalignant dysplasia or adenoma (Figures 3D and 3E). There were few islets with infiltrating $CD4^+$ and $CD8^+$ T cells, and destruction inside the islets was rare (Figures 1E and 3E). Islets of Tag-Th1-treated mice had only very small vessels, and even the somewhat larger adenomas were almost devoid of vascular structures or α-actin-expressing pericytes (Figures 3D and 3E).

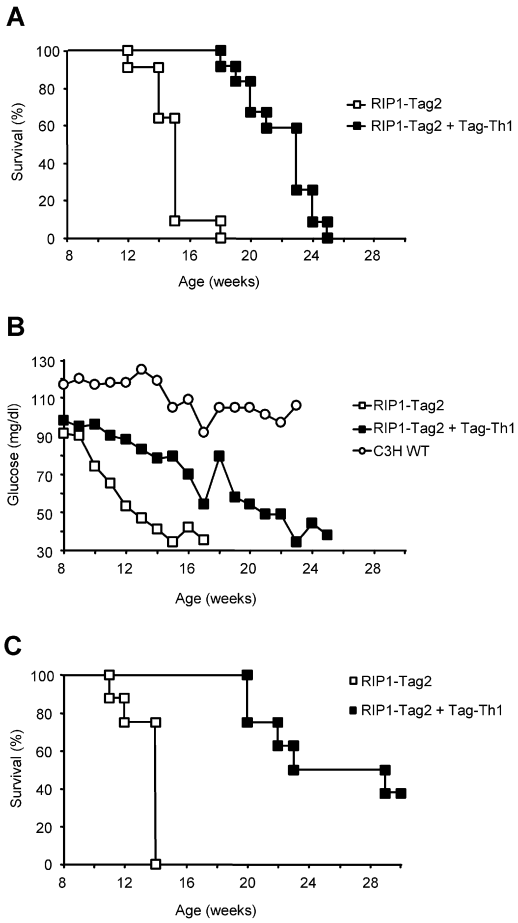

Figure 2. Adoptive Transfer of Tag-Th1 Cells Extends Life of RIP1-Tag2 Mice without Causing Diabetes

(A) Survival of sham-treated RIP1-Tag2 mice or RIP1-Tag2 mice receiving 10^7 Tag-Th1 cells once every week ($n = 11$, $p < 0.0005$), with treatment starting at week 7.

(B) Corresponding blood glucose levels of RIP1-Tag2 mice, RIP1-Tag2 mice receiving Tag-Th1 cells, or C3H wild-type mice. The data show the curves of one representative experiment.

(C) Survival of sham-treated RIP1-Tag2 mice or RIP1-Tag2 mice receiving 10^7 Tag-Th1 cells once every week ($n = 8$, $p < 0.001$), with treatment starting at week 5.

Tag-Th1 Cells Prevent Aberrant $\alpha_v\beta_3$ Activation and Tumor Vessel Formation

To quantify the histological finding that Tag-Th1 cells prevented the angiogenic switch and inhibited blood vessel formation, we first counted tumors and determined tumor size in relation to the pancreas and the number of $CD31^+$ vessels using morphometric techniques. At week 14, sham-treated RIP1-Tag2 mice

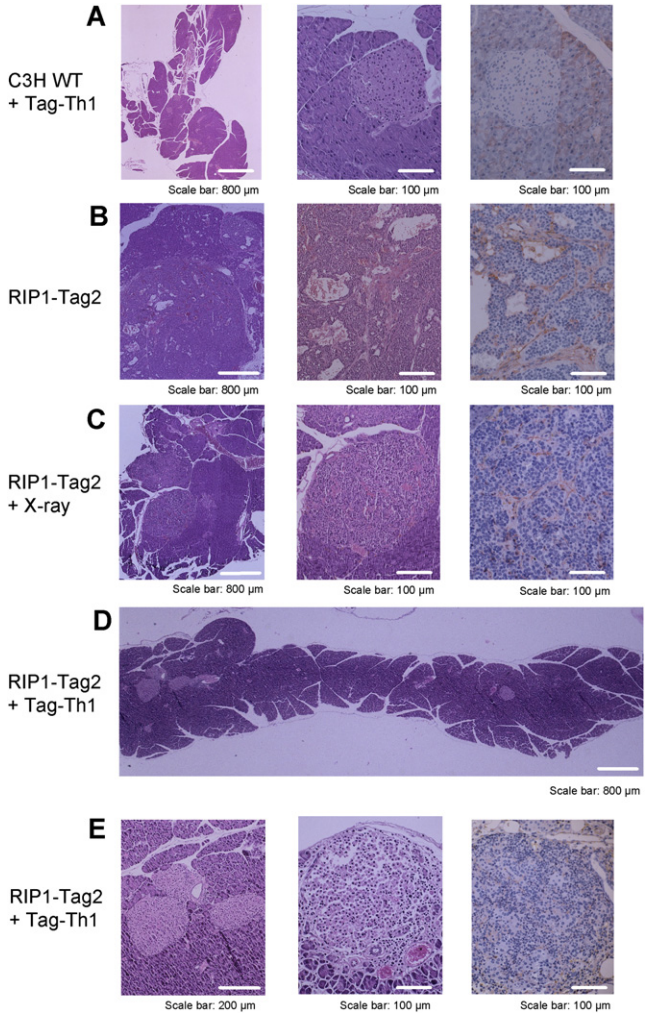

Figure 3. Tag-Th1 Cells Prevent Growth of Endogenous Tumors and Angiogenesis in Transgenic RIP1-Tag2 Mice

(A) H&E staining of pancreas (left) or islets (center), and mature vessels stained with anti-α-actin antibody (right) from a C3H wild-type mouse treated with Tag-Th1 cells.

(B and C) H&E staining of pancreas (left), islet carcinomas (center) or α-actin-staining (right) of an islet carcinoma from an untreated RIP1-Tag2 mouse (B) or after low-dose irradiation (2 Gy) (C).

(D and E) H&E staining of total pancreas ([D], detail; [E], left) or an infiltrated islet adenoma ([E], center), or α-actin staining ([E], right) of an islet adenoma from Tag-Th1 cell-treated RIP1-Tag2 mice with treatment starting at week 7.

(A–E) The age of the mice was 12 weeks ± 4 days.

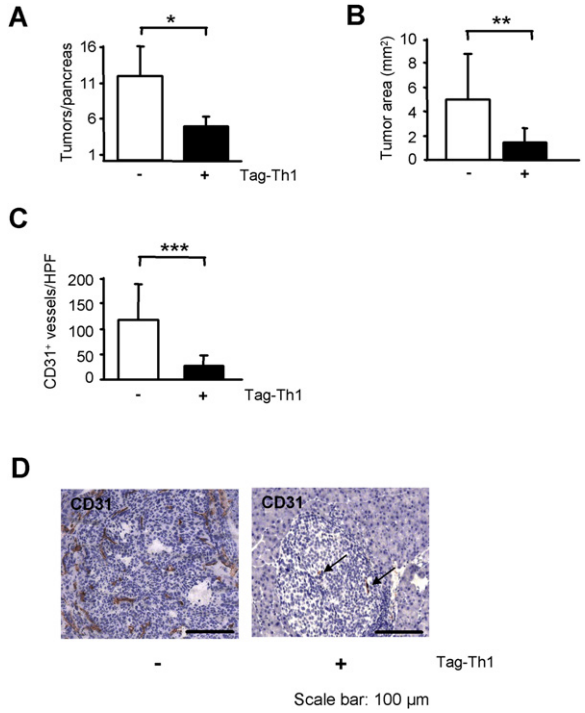

Figure 4. Tag-Th1 Cells Prevent Tumor Vessel Growth and the Angiogenic Switch

(A) Mean values ± SD of tumor counts of sham-treated RIP1-Tag2 mice (white; n = 18) or Tag-Th1 cell-treated RIP1-Tag2 mice (black; n = 11). *p = 0.002.

(B) Cumulative area of the three largest tumors (mean ± SD) of sham-treated RIP1-Tag2 mice (white; n = 18) or Tag-Th1-treated RIP1-Tag2 mice (black; n = 11). **p = 0.006.

(C) Numbers ± SD of $CD31^+$ vessels in ten high-power fields (HPF) in tumors derived from sham-treated RIP1-Tag2 (white; n = 18) or RIP1-Tag2 mice treated with Tag-Th1 cells (black; n = 11). ***$p < 0.001$.

(D) Immunohistochemistry of $CD31^+$ endothelial cells of vessels in sham-treated (left) or RIP1-Tag2 mice treated with Tag-Th1 cells (right). Arrows point to $CD31^+$ small vessels. Age: 13 weeks.

developed about 11 tumors, two to three being large tumors with prominent angiogenesis. At this time, Tag-Th1 cell-treated mice had fewer adenomas/tumors (Figure 4A), and the tumors were significantly smaller (Figure 4B) and also had significantly fewer vessels than those in sham-treated mice (Figure 4C). CD31 and α-actin staining revealed that the few vessels developing in adenomas of Tag-Th1 cell-treated mice were small and displayed normal $CD31^+$ endothelia and pericytes (Figure 4D and data not shown). In contrast, only part of the tumor vessels in sham-treated mice expressed both markers of vessel maturation. Large tumors of sham-treated mice showed numerous immature vascular structures devoid of $CD31^+$ endothelia or α-actin$^+$ pericytes and microhemorrhaging (Figure 4D and data not shown).

As vessels sprouting inside tumors strongly express activated $\alpha_v\beta_3$ integrin (Carmeliet and Jain, 2000), we determined the presence and distribution of β_3 integrin by immunohistology. The β_3 integrin staining was restricted to endothelia lining vessels inside the carcinomas, and tumor cells did not express β_3 integrin (Figures 5A and 5B). β_3 integrin$^+$ endothelia established large tubules in tumors of sham-treated mice, while β_3 integrin$^+$ vessels were rare and very small in islets of RIP1-Tag2 mice treated with Tag-Th1 cells (Figure 5B). Thus, the analysis of $\alpha_v\beta_3$ integrin expression inside the tumor vessels provides the opportunity to quantify active tumor angiogenesis.

We addressed this question with Gluco-RGD, a pentapeptide that selectively binds with high affinity to activated $\alpha_v\beta_3$ integrin (Haubner et al., 2001; Pfaff et al., 1994). In agreement with the early angiogenesis seen in histology, [^{125}I]Gluco-RGD uptake was slightly increased in some of the premalignant dysplasias of 7-week-old RIP1-Tag2 mice (Figures 5C and 5D). During the following 3 weeks, [^{125}I]Gluco-RGD uptake increased 4- to 5-fold and reached a plateau around week 9 (Figure 5D).

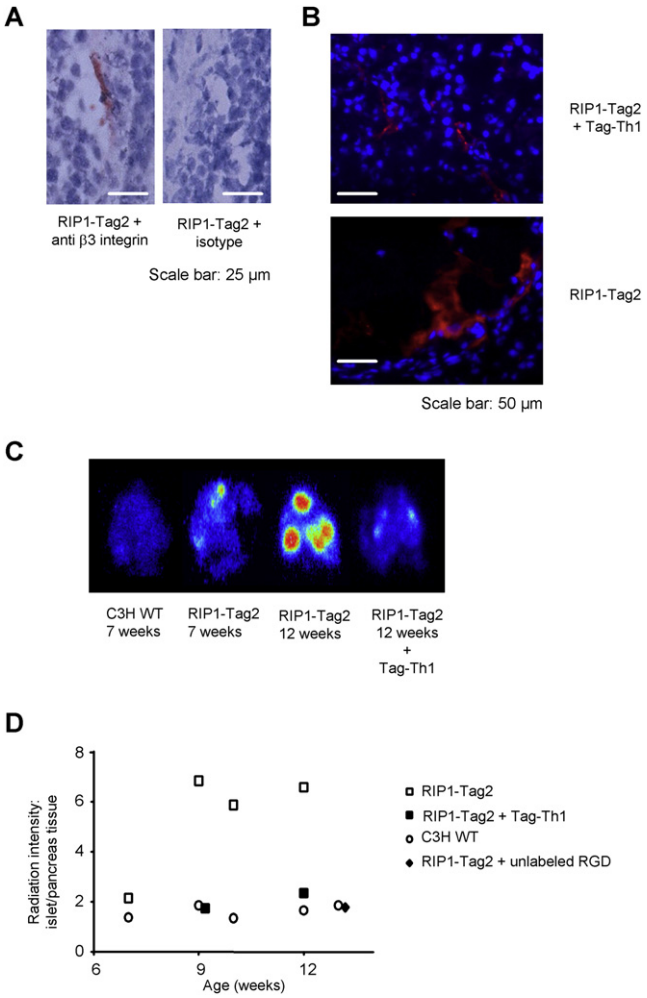

Figure 5. Tag-Th1 Cells Prevent Development of Integrin $\alpha_v\beta_3$-Expressing Endothelial Cells and Tumor Vessels

(A) Immunohistochemistry of tumor vessel-lining endothelia with β_3 mAb (left) or isotype control (right) in a RIP1-Tag2 mouse (12 weeks).

(B) β_3-immunohistochemistry of tumor vessels in a RIP1-Tag2 mouse (8 weeks) treated with Tag-Th1 cells (top) or an untreated RIP1-Tag2 (bottom).

(C) Phosphor storage autoradiography of the pancreas of a C3H (7 weeks), a RIP1-Tag2 (7 weeks), an untreated RIP1-Tag2 (12 weeks), and a RIP1-Tag2 mouse (12 weeks) treated with Tag-Th1 cells. The autoradiography was performed 3 hr after injection of 370 kBq [^{125}I]Gluco-RGD.

(D) Mean radiation intensity of [^{125}I]-Gluco RGD uptake in pancreata of C3H, untreated RIP1-Tag2 and RIP1-Tag2 mice treated with Tag-Th1 cells (n = 3). Selectivity was demonstrated by blocking [^{125}I]-Gluco-RGD uptake with unlabeled c(RGDfV) peptide.

[^{125}I]Gluco-RGD enriched only inside vascularized carcinomas (Figure 5C), and its binding to $\alpha_v\beta_3$ was receptor specific, as it was blocked by pretreatment with unlabeled c(RGDfV) peptide (Figure 5D). In contrast to sham-treated mice, $\alpha_v\beta_3$ integrin activation was almost prevented in islets of mice treated with Tag-Th1 cells (Figures 5C and 5D). At 9 to 12 weeks of age, [^{125}I]Gluco-RGD binding in these mice stayed at the starting level of untreated, 7-week-old mice (Figures 5C and 5D), demonstrating that Tag-Th1 cells arrested tumor angiogenesis. Tag-Th1 cells did not affect [^{125}I]Gluco-RGD uptake in any other tissue, such as the gut (data not shown).

Tag-Th1 Cells Arrest Tumor Cell Proliferation without Destroying TAA-Expressing Islets

To exclude that inhibition of angiogenesis resulted from tumor cell destruction by CTL that were activated by Tag-Th1 cells, we deleted >98% CD8$^+$ cells by weekly injection of monoclonal antibody (mAb) RmCD8-2 (Egeter et al., 2000), starting 1 week before therapy. Even in the absence of CTL, [^{125}I]Gluco-RGD uptake remained at background levels in Tag-Th1 cell-treated mice (Figures 6A and 6B), demonstrating that inhibition of tumor angiogenesis by Tag-Th1 cells was CTL independent.

Th1 cells might also control tumor growth by inducing extensive apoptosis of TAA-expressing tumor cells or of endothelia lining the tumor vessels through IFN-γ- and TNF-mediated signals. We therefore analyzed the number of apoptotic tumor cells or endothelial cells in Tag-Th1 cell-treated or untreated RIP1-Tag2 mice at week 8, the time when carcinomas start to develop in untreated RIP1-Tag2 mice. Most islets or endothelia of untreated RIP1-Tag2 mice displayed only few apoptotic cells (3.4% ± 0.9% [n = 4] TUNEL$^+$ islet cells). Importantly, Tag-Th1 cell-treated mice did not show a significant increase in apoptotic cells (2.7% ± 0.6% [n = 4] TUNEL$^+$ islet cells; for TUNEL staining of islets see Figure 6C). Thus, apoptosis induction is unlikely to account for the therapeutic effect of Tag-Th1 cells.

Alternatively, Tag-Th1 cells may inhibit tumor cell proliferation. To address this question, BrdU was injected into mice, and the pancreas was stained to quantify proliferating β cells. Tumor-bearing mice had strongly increased numbers of BrdU$^+$ cells as compared to C3H mice (Figure 6D). Treatment with Tag-Th1 cells significantly reduced BrdU$^+$ tumor cells (Figure 6D), while irradiation alone did not.

In the Absence of Tightly Coordinated IFN-γ and TNF Interactions, Tag-Th1 Cells Promote Tumor Growth and Angiogenesis

Proinflammatory in vivo functions of Th1 cells strictly depend on the coordinated interaction of IFN-γ and TNF (Abbas et al., 1996). Based on this observation, we treated RIP1-Tag2 mice with Tag-Th1 cells in the presence of anti-IFN-γ mAb or control mAb. In the absence of Tag-Th1 cells, anti-IFN-γ mAb had no clear effects on tumor growth (Figure S3). In sharp contrast, when we injected identical doses of anti-IFN-γ together with Tag-Th1 cells, decline of blood glucose and death occurred as rapidly as in sham-treated mice (Figure 7A; Figure S4). Anti-IFN-γ did not delete Tag-Th1 cells, as spleens of anti-IFN-γ-treated mice had normal numbers of idiotypic Tag-Th1 cells (Figure 7B) that produced decreased amounts of IFN-γ. In the presence of anti-IFN-γ, fluorescence-labeled Tag-Th1 cells homed normally into the pancreas and draining lymph node of RIP1-Tag2 mice (Figure S5). At 14 weeks, mice treated by a combination of Tag-Th1 cells and anti-IFN-γ had a 2-fold greater tumor burden than untreated mice due to increased tumor size (Figures 7C and 7D). Increased tumor size closely correlated with significantly increased tumor vessel density (Figure 7E). In some mice, tumor vessels grew so rapidly that islet carcinomas protruded into the abdomen (Figure 7C) or caused metastasis, phenomena that we never observed in more than 100 sham-treated RIP1-Tag2 mice.

Then, we analyzed the effects of IFN-γ on interferon-inducible protein 10 (IP10; CXCL10) or monokine-induced by IFN-γ (Mig;

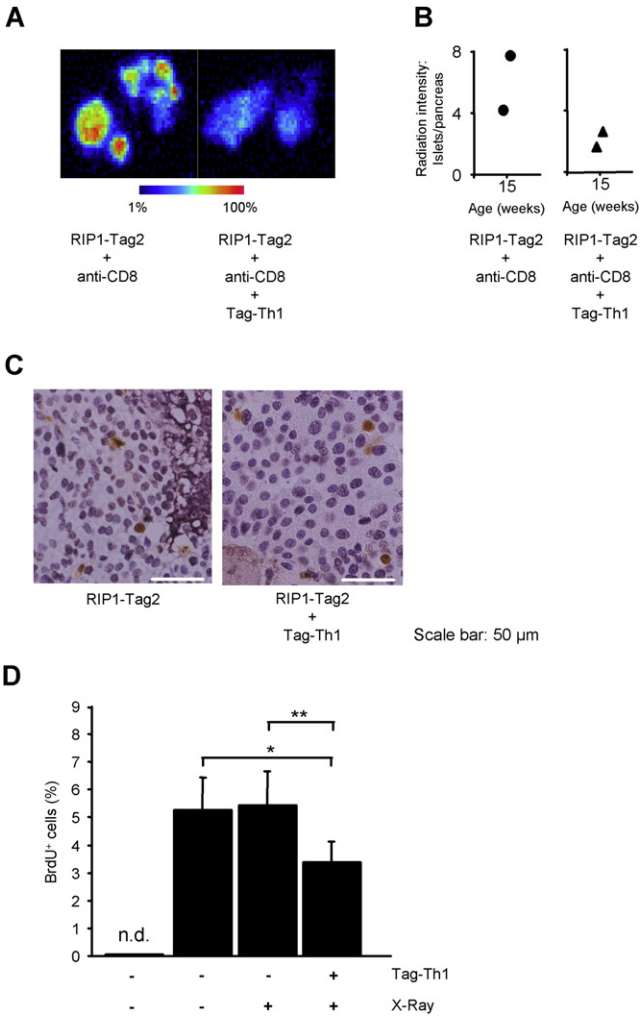

Figure 6. Inhibition of Multistage Carcinogenesis by Tag-Th1 Cells Is Independent of Host CD8-Positive Cells and Tumor Cell Apoptosis but Reduces Proliferation inside Adenomas

(A) Phosphor storage autoradiography of pancreata of CD8-depleted RIP1-Tag2 mice (15 weeks). Mice were untreated or received weekly injections of Tag-Th1 cells.

(B) Corresponding mean radiation intensity of [^{125}I]Gluco-RGD uptake in pancreata of untreated RIP1-Tag2 (left) or RIP1-Tag2 mice treated with Tag-Th1 cells (right). Two independent experiments are shown.

(C) TUNEL (brown) and α-actin staining (red) of insulinomas at 8 weeks of Tag-Th1 cell-treated (right, 2 weeks of treatment) or sham-treated RIP1-Tag2 mice (left).

(D) BrdU$^+$ cells in % ± SD (n = 4) in islets of controls (nontransgenic mice, left bar), or sham-treated RIP1-Tag2 mice with or without additional X-ray treatment, or RIP1-Tag2 mice treated with Tag-Th1 lymphocytes. *p = 0.03; **p = 0.02; n.d. = not detectable. Age: 8 weeks; 2 weeks of treatment.

CXCL9), two potent angiogenesis inhibitors (Tannenbaum et al., 1998). On week 14, the pancreas of Tag-Th1 cell-treated mice expressed 10-fold higher mRNA levels of CXCL9 and CXCL10 than the pancreas from C3H or sham-treated RIP1-Tag2 mice (Figure 7F). In the presence of anti-IFN-γ, Tag-Th1 cells failed to induce either CXCL9 or CXCL10 (Figure 7F), showing that Tag-Th1 cells induced the two chemokines through an IFN-γ-dependent mechanism. In contrast, mRNA levels of vascular endothelial growth factor (VEGF) or matrix metallo-proteinase (MMP)9 remained unaffected by Tag-Th1 cells (data not shown).

As the proinflammatory effects of TNF require signaling through TNFR1, we backcrossed *TNFR1*$^{-/-}$ mice (Pfeffer et al., 1993) over 12 generations to the C3H background and crossed them with RIP1-Tag2 mice to generate *TNFR1*$^{-/-}$ × RIP1-Tag2 mice. In untreated *TNFR1*$^{-/-}$ × RIP1-Tag2 mice, blood glucose decreased somewhat slower than in normal RIP1-Tag2 mice or heterozygous *TNFR1*$^{-/+}$ × RIP1-Tag2 mice. Mean survival of untreated *TNFR1*$^{-/-}$ × RIP1-Tag2 mice was also slightly prolonged (data not shown), suggesting that TNFR1-mediated signals facilitate multistage carcinogenesis in RIP1-Tag2 mice. To study Tag-Th1 cells, we started by imaging Th1 cell migration. In *TNFR1*$^{-/-}$ × RIP1-Tag2 mice, Tag-Th1 cells showed the same distribution as in TNFR1-expressing mice and survived normally (Figures S6 and S7).

Surprisingly, when treated with Tag-Th1 cells, *TNFR1*$^{-/-}$ × RIP1-Tag2 mice died faster than *TNFR1*$^{+/+}$ × RIP1-Tag2 mice, and Tag-Th1 cell-treated *TNFR1*$^{-/-}$ × RIP1-Tag2 mice died even faster than sham-treated *TNFR1*$^{-/-}$ × RIP1-Tag2 mice (Figure 8A). To quantify the enhancement of tumor growth by Tag-Th1 cells in *TNFR1*$^{-/-}$ × RIP1-Tag2 mice, we counted the islet cells of sham-treated *TNFR1*$^{-/-}$ × RIP1-Tag2 mice and of *TNFR1*$^{-/-}$ × RIP1-Tag2 mice treated with Tag-Th1 cells. In *TNFR1*$^{-/-}$ × RIP1-Tag2 mice, Tag-Th1 cells increased the number of islet cells 10-fold, as compared to sham-treated mice (Figure 8B). To determine the reasons of enhanced tumor growth, we analyzed antiangiogenic chemokines and tumor cell proliferation in vivo. While Tag-Th1 cells strongly induced the expression of CXCL9 and CXCL10 in TNFR1-expressing RIP1-Tag2 mice, both chemokines were at background in Tag-Th1 cell-treated *TNFR1*$^{-/-}$ × RIP1-Tag2 mice (Figure 8C). Finally, we determined BrdU-labeled cells in Tag-Th1 cell-treated and sham-treated *TNFR1*$^{-/-}$ × RIP1-Tag2 mice. Tag-Th1 cells significantly increased proliferating tumor cells in *TNFR1*$^{-/-}$ × RIP1-Tag2 mice (Figure 8D). Thus, the same Tag-Th1 cells that efficiently suppressed angiogenesis, tumor cell proliferation, and multistage carcinogenesis under normal experimental conditions strongly promoted Tag-driven tumor development in mice with impaired IFN-γ signaling or TNFR1 signaling.

DISCUSSION

Studying the effects of adaptive immunity on endogenous multistage carcinogenesis developing under the pressure of deregulated p53 and Rb protein, we found that TAA-specific Th1 cells homed in the peritumoral microenvironment, where they arrested angiogenesis, cell proliferation, and multistage carcinogenesis. This inhibition was independent of CTL or signs of tumor cell killing. In the absence of either IFN-γ signaling or TNFR1 signaling, the same T cells promoted multistage carcinogenesis.

Both innate and adaptive immune responses exert opposing effects on the growth of various experimental and human tumors (Arnott et al., 2004; Daniel et al., 2003; de Visser et al., 2006; Koebel et al., 2007; Lin and Karin, 2007; Moore et al., 1999; Prehn, 1972; Siegel et al., 2000; Schadendorf et al., 2006; Schultz et al., 2004; Suganuma et al., 2006). However, the conditions distinguishing tumor promotion from tumor suppression are poorly understood.

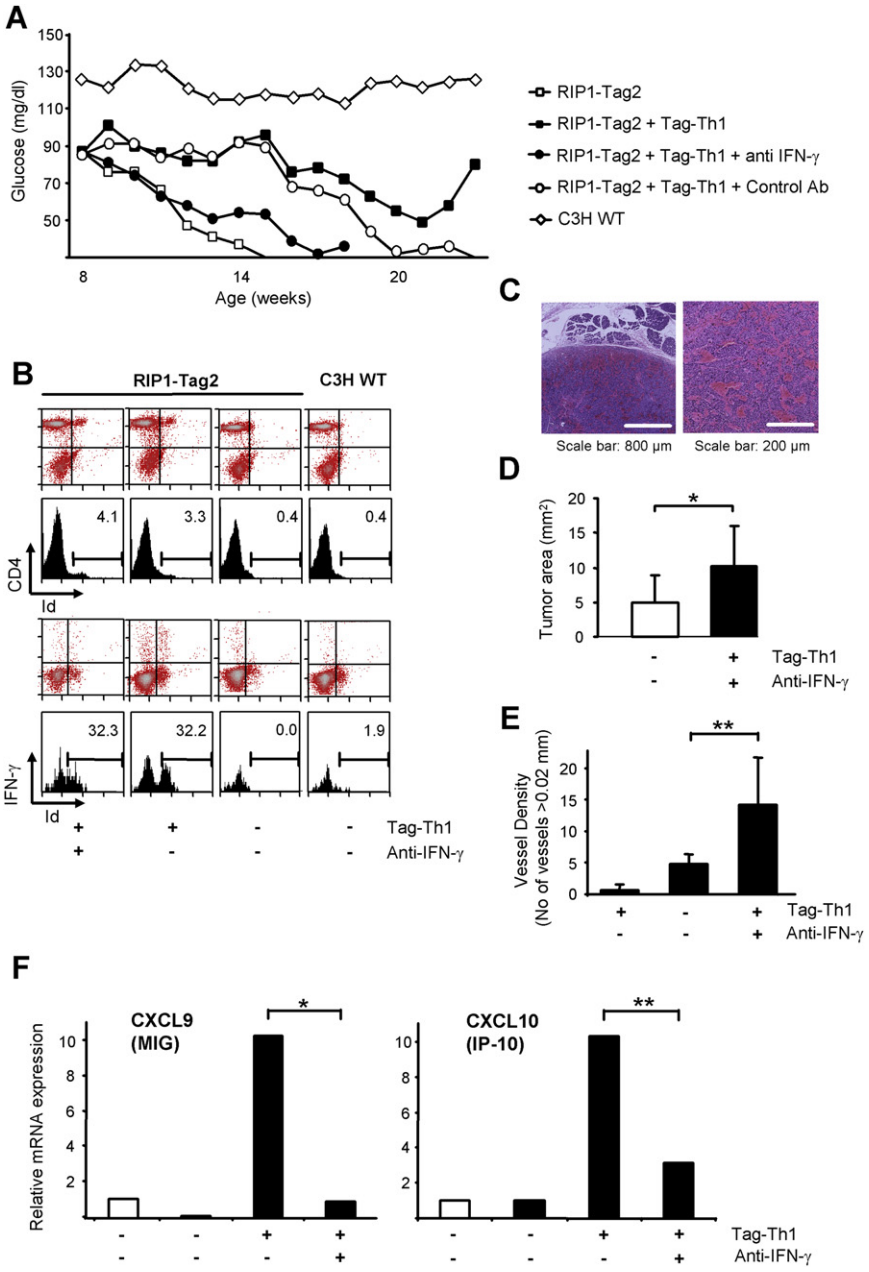

Figure 7. In the Absence of IFN-γ, Tag-Th1 Cells Paradoxically Promote Multistage Carcinogenesis

(A) Blood glucose in Tag-Th1-treated RIP1-Tag2 mice in the presence of blocking anti-IFN-γ mAb (weekly injection of mAb XMG12 [Egeter et al., 2000]) (n = 5) or control mAb (n = 4, $p < 0.005$).

(B) FACS analysis of $CD4^+$ and Tag-Th1-idiotype$^+$ cells in spleens of RIP1-Tag2 mice (12 weeks), treated with Tag-Th1 cells in the presence or absence of IFN-γ mAb (top). (Bottom) Intracytoplasmatic IFN-γ load of Tag-Th1-idiotype$^+$ spleen cells.

(C) Overview (left) and high-power field (right) of H&E-stained islet carcinomas in a RIP1-Tag2 mouse (14 weeks) treated with Tag-Th1 cells and anti-IFN-γ mAb.

(D) Cumulative area of the three largest tumors of sham-treated RIP1-Tag2 (14 weeks, mean ± SD, n = 8) or RIP1-Tag2 mice treated with Tag-Th1 and IFN-γ antibody (n = 15). *p = 0.02.

(E) Vessel density (number of vessels ± SD) in Tag-Th1 (n = 3)- or sham (n = 8)-treated RIP1-Tag2, or in RIP1-Tag2 mice (14 weeks) treated with Tag-Th1 cells and anti-IFN-γ mAb. **p = 0.01.

(F) Quantitative RT-PCR of CXCL9 and CXCL10 in the indicated groups (n = 4–7) of mice. The white bar represents C3H. CXCL9 and CXCL10 mRNA expression were normalized to aldolase. *p = 0.01 for CXCL9, and **p = 0.02 for CXCL10.

Analysis and interpretation of immune responses on tumor development require consideration of the tumor analyzed and the cytokine conditions studied. Transplanted tumors, tumors induced by carcinogens, or tumors developing as a consequence of deregulated apoptosis and clearance mechanisms may show opposing effects to immune responses (de Visser et al., 2006). Thus, calcineurin inhibitors strongly increase the risk of virally or UV-induced malignancies (Haagsma et al., 2001), while they may protect against other types of cancer, such as breast cancer (Stewart et al., 1995).

Similarly, the action of cytokines critically depends on their concentration, the time of action, the target cell, and their coordination. High TNF doses that act for short periods of time induce apoptosis of tumor vessels and tumor necrosis, an effect used as therapy for melanoma metastases (Carswell et al., 1975; Olieman et al., 1999; Stoelcker et al., 2000). In contrast, continuous low doses of TNF promote early steps of tumor development, such as tumor angiogenesis in chemically or UV-induced carcinomas (Arnott et al., 2004; Moore et al., 1999; Suganuma et al., 1999). In line with this, islet carcinomas developed slower in *TNFR1*$^{-/-}$ × RIP1-Tag2 mice than in TNFR1-expressing litters. Yet, in the presence of Tag-Th1 cells, the same signaling defect converted from a tumor-protective into a tumor-promoting property. Similarly, IFN-γ exerts potent antitumor effects under most conditions. Yet, persistent inflammation mediated by IFN-γ-producing $CD4^+$ T cells promotes the development of skin tumors in mice expressing the human papilloma virus type 16 early regions gene (Daniel et al., 2003). Moreover, IFN-γ may attenuate its own action by promoting Th1 cell suicide (Berner et al., 2007).

IFN-γ or IFN-γ-producing Th1 cells protect against malignancies under many conditions, and multiple mechanisms have been proposed to mediate the tumor-protective effects of IFN-γ. IFN-γ may directly inhibit growth of tumor cells and seems to enhance the natural tumor immune surveillance against virus-induced tumors (Billiau, 1996; Boehm et al., 1997; Kaplan et al., 1998; Koebel et al., 2007; Shankaran et al., 2001; Street et al., 2002). IFN-γ is needed for activation of APC by NK cells

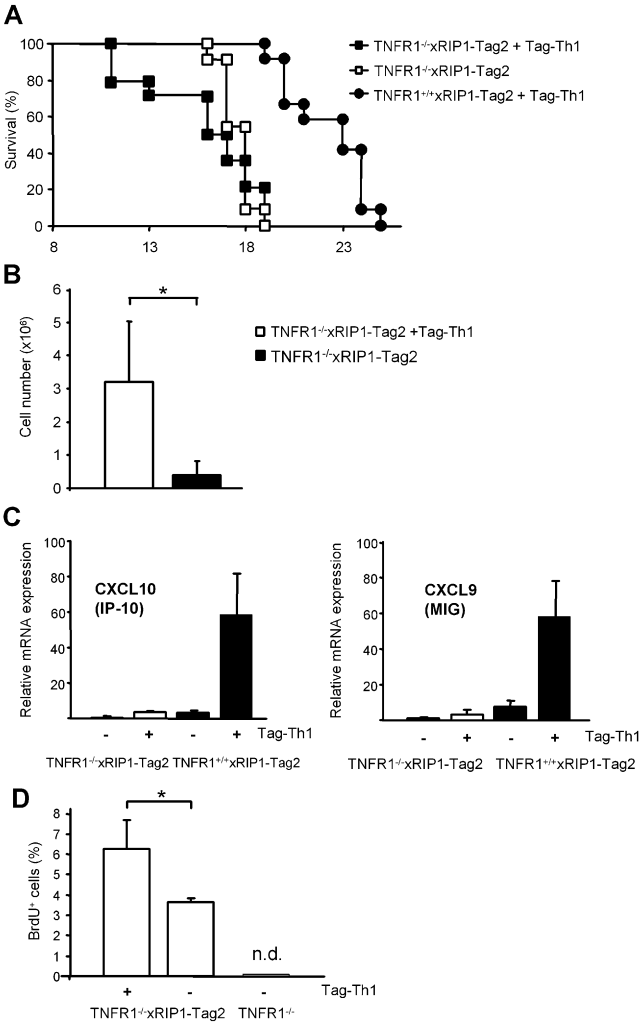

Figure 8. In the Absence of TNFR1 Signaling, Tag-Th1 Cells Promote Multistage Carcinogenesis

(A) Survival of sham-treated *TNFR1*$^{-/-}$ × RIP1-Tag2 (n = 12), *TNFR1*$^{-/-}$ × RIP1-Tag2 mice treated with Tag-Th1 cells (n = 11) or *TNFR*$^{+/+}$ × RIP1-Tag2 mice treated with Tag-Th1 cells (n = 5). $p < 0.001$ for the difference in survival between *TNFR1*$^{-/-}$ × RIP1-Tag2 mice and *TNFR*$^{+/+}$ × RIP1-Tag2 both treated with Tag-Th1 cells, and $p = 0.05$ for the difference between sham-treated *TNFR1*$^{-/-}$ × RIP1-Tag2 mice and *TNFR1*$^{-/-}$ × RIP1-Tag2 mice treated with Tag-Th1 cells.

(B) Tumor cell number ± SD (n = 3) after collagenase/trypsin digestion of pancreata of sham-treated *TNFR*$^{-/-}$ × RIP1-Tag2 (black) or *TNFR1*$^{-/-}$ × RIP1-Tag2 mice treated with Tag-Th1 cells (white). *p = 0.04.

(C) Quantitative real-time RT-PCR ± SD (n = 3) of CXCL9 and CXCL10 in the indicated groups of mice. CXCL9 and CXCL10 mRNA expression were normalized to aldolase.

(D) BrdU^{+} cells in % ± SD (n = 4) in islets of *TNFR1*$^{-/-}$ × RIP1-Tag2 mice treated with Tag-Th1 lymphocytes or sham-treated *TNFR1*$^{-/-}$ × RIP1-Tag2 mice, or in islets of single transgenic *TNFR1*$^{-/-}$ mice (n.d. = not detectable). *p = 0.03.

(Garcia-Lora et al., 2003; Mocikat et al., 2003; Zitvogel, 2002), activation of cytotoxic macrophages, and rejection of transplanted MHC class II-positive or MHC class II-negative tumor cells by Th1 cells (Chamoto et al., 2006; Daniel et al., 2005; Egeter et al., 2000; Greenberg, 1991; Qin and Blankenstein, 2000) and can prevent vessel outgrowth from the host stroma into transplanted tumors (Qin and Blankenstein, 2000; Spiotto et al., 2004). IFN-γ may also interfere with signal cascades that are involved in malignant transformation, such as c-Myc-, p53-, or Rb-dependent pathways (Agrawal et al., 2002; Ramana et al., 2000). Yet, the effects of IFN-γ- and TAA-specific Th1 cells on the various steps of multistage carcinogenesis are poorly understood. It seems that TAA-specific Th1 responses are most effective if induced prior to or at very early stages of tumor development (Holmgren et al., 2006; Nanni et al., 2001; Pannellini et al., 2006; Willimsky and Blankenstein, 2005).

In a functionally related but biologically different tumor model, the RIP1-Tag5 mouse, control of tumor growth by CTL-mediated tumor cell killing is followed by restoration of normal blood vessels in the pancreatic islets. These data suggest a direct relation between tumor cell destruction by CTL and vessel architecture (Ganss et al., 2002; Garbi et al., 2004; Otahal et al., 2006). Our results point toward a fundamentally different interpretation. They revealed that Tag-Th1 cells inhibited angiogenesis and multistage carcinogenesis without significant tumor cell destruction. This was surprising, as Th1 cells can induce both apoptosis in tumor cells (Egeter et al., 2000) and destructive autoimmune disease (Racke et al., 1994). Molecular analysis of tumors and of the microenvironment revealed that Th1 cells primarily migrated into the peritumoral microenvironment, and that neither treatment with Tag-Th1 cells nor inhibition of TNFR1 or IFN-γ signaling affected VEGF or MMP9 mRNA expression.

The combined action of IFN-γ signaling and TNFR1 signaling was needed to prevent activation of $\alpha_v\beta_3$ integrin, tumor-angiogenesis, and multistage carcinogenesis, at least in part indirectly through induction of the antiangiogenic chemokines CXCL9 and CXCL10. One potentially relevant source of the two chemokines are APC (unpublished data). These angiogenesis inhibitors must obviously overcome tumor-promoting factors delivered by the Tag-Th1 cell-mediated inflammation. Possible promoters of tumor angiogenesis delivered during Th1 cell-mediated inflammation are IL-17, CSF1, TNF, MMP9, or VEGF. This interpretation of Th1 cell action on tumor development is in agreement with the observation that accelerating the angiogenic switch also accelerates multistage carcinogenesis (Inoue et al., 2002). Thus, our findings are best conceivable with a model in which the combined action of IFN-γ signaling (Indraccolo et al., 2007) and TNFR1 signaling on endothelia induces tumor dormancy at least in part through antiangiogenic chemokines that arrest or delay tumor angiogenesis and subsequent multistage carcinogenesis, even in the presence of VEGF and MMP9. The role of Th1 cells in preventing multistage carcinogenesis is more complex than simple inhibition of $\alpha_v\beta_3$ integrin activation by the combined delivery of TNF and IFN-γ (Ruegg et al., 1998).

To precisely follow tumor angiogenesis, we studied vessel formation and tumor development by histology, immune histology, and objectively quantified activated $\alpha_v\beta_3$ integrin, utilizing Gluco-RGD that binds with high affinity selectively to activated $\alpha_v\beta_3$ integrin (Haubner et al., 2001; Pfaff et al., 1994). Gluco-RGD may also bind to $\alpha_5\beta_1$, or $\alpha_{II}\beta_3$ integrin, but with much lower affinity (Haubner et al., 2001; Pfaff et al., 1994). As β_1 and β_3 integrins are only expressed by endothelia and not by tumor cells (Baluk et al., 2003; Yao et al., 2006), quantitative analysis thus reflects the extent of active tumor angiogenesis. This quantification

revealed that the rate of newly built vessels increased 5-fold during the transition of premalignant dysplasias and adenomas into carcinomas and that Tag-Th1 cells prevented this aberrant activation of $\alpha_v\beta_3$ integrin and tumor angiogenesis.

As in the absence of either IFN-γ signaling or TNFR1 signaling tumor-protective Th1 cells strongly enhanced multistage carcinogenesis, future development of tumor immune therapy must take into account that T cell-derived cytokines can directly interfere with multistage carcinogenesis, or even with the natural development of tumors that evolve under the pressure of impaired tumor suppressors, such as p53 or Rb. The direct impact of our findings for humans results from recent melanoma vaccine trials, where protection from metastasis was associated with the appearance of IFN-γ-producing T cells. In the same cohort, metastases expanded more rapidly than in controls, if patients failed to develop IFN-γ-producing T cells (e.g., Schadendorf et al., 2006; Schultz et al., 2004).

EXPERIMENTAL PROCEDURES

Animals

Animal experiments were approved by the Animal Care Committee (AZ 211-2531-63/98 and HT 2/03). C3H mice from Charles River (Sulzberg, Germany), transgenic RIP1-Tag2, double transgenic *TNFR1*$^{-/-}$ × RIP1-Tag2 (backcross of *TNFR1*$^{-/-}$ mice over 12 generations to C3H), and TCR2 mice all on a C3H background were bred under specific pathogen-free conditions.

Cell Culture and Single-Cell Analysis

CD4$^+$ T cells were isolated from TCR2 mice and cultured for 1 week with Tag peptide 362-384, CpG-DNA 1668, and anti-IL-4 mAb to induce Th1 cells as described (Egeter et al., 2000). Cells were restimulated with ionomycin and phorbol-myristate-acetate (Sigma, Munich, Germany) in vitro in the presence of brefeldin A (PharMingen, Heidelberg, Germany). Surface staining with fluorescein-labeled mAb to the TCR idiotype and intracellular staining with phycoerythrin-labeled mAb to IL-4 or IFN-γ or isotype controls (PharMingen) was done according to the manufacturer's protocol. Cells were analyzed on a BD FACScan cytometer (Becton Dickinson [BD], Heidelberg, Germany).

Treatment with Radiation and Tag-Th1 Cells

Before the first therapy and thereafter every 4–6 weeks, all mice received 2 Gy total-body irradiation. Sham-treated mice received 0.9% NaCl solution, while Tag-Th1 cell-treated RIP1-Tag2 mice received 10^7 Tag-Th1 cells in 0.9% NaCl/week intraperitoneally starting at week 5 or 7. CD8 cells were depleted, and IFN-γ was blocked by weekly injection of mAbs as described (Mocikat et al., 2003). CD8$^+$ cells were reduced >98%.

Determination of Blood Glucose

Blood glucose was determined using an Eppendorf EBIO plus Glucose-Analyzer (Eppendorf, Hamburg, Germany).

Isolation of Insulinomas

After collagenase digestion (1 mg/ml; Serva, Heidelberg, Germany) for 10 min at 37°C, islets were isolated from exocrine tissue under binoculars.

BrdU Labeling

For identification of proliferating cells, RIP1-Tag2 mice were injected with 200 mg/kg body weight BrdU (Sigma) and sacrificed 1–2 hr later. Paraffin-embedded slides were deparaffinized and hydrated in graded alcohols. Slides were then boiled in a antigen retrieval solution (BD) and incubated overnight with rat anti-BrdU mAb (BD) at a dilution of 1:10 for 1 hr at 23°C. Slides were rinsed with PBS and treated with streptavidin-horseradish-peroxidase (BD) for 30 min. After rinsing, slides were treated with 3,3′-diaminobenzidine (DAKO, Hamburg, Germany) for up to 10 min. Slides were counterstained in hematoxylin and mounted under a glass coverslip. Cells labeled with BrdU displayed brown nuclear stain (positive control: duodenum from mice; negative controls: insulinomas incubated with a nonspecific antibody).

For quantitation, a minimum of 1000 β cells per mouse were evaluated and individual tumors were counted separately.

Histology and Immunohistology

Serial paraffin or cryostat sections (5–7 μm) were stained with hematoxylin and eosin (H&E), mAb to α-actin (Roche, Mannheim, Germany), β_3 integrin (PharMingen), CD31 (PharMingen), or isotype Ab (Roche and PharMingen) as described (Biedermann et al., 2001). The scale was either measured or estimated and given in micrometers. TdT-mediated dUPT nick end labeling (TUNEL) staining was performed using the ApopTag apoptosis kit (Serologicals, Norcross, CA).

Quantitation of Vessel Density

The number of CD31-positive vessels (vessel density) or α-actin-positive vessels was counted in three tumors per pancreas. For determination of α-actin- and CD31-negative tumor blood vessels, all vessels with a lumen ≥0.02 mm were counted (n = 3 tumors/mouse).

Assessment of Tumor Burden and Tumor Numbers

Cryostat sections (5 μm) were obtained from snap-frozen pancreata. Sections were H&E stained. Length and width of each pancreas tumor were measured microscopically. The formula 0.5 width × 0.5 length × π for approximating the area was applied, and the sum of the three largest tumor areas per pancreas was given.

Molecular Analysis

Tissues were mechanically homogenized in lysis buffer (RNeasy kit; QIAGEN, Hilden, Germany). During RNA purification genomic DNA was digested with RNAase-free DNAase (QIAGEN). Total RNA (2 μg) were reverse transcribed (Omniscript RT-kit, QIAGEN). For each primer pair a standard curve was developed, and mRNA expression levels were determined by real-time PCR and normalized with the expression level of aldolase. The following primers were used: Aldolase (amplicon length 571 bp): FP, 5′-AGCTGTCTGACATCGCTCACCG; RP, 5′-CACATACTGGCAGCGCTTCAAG; CXCL9 (256 bp): FP, 5′-TCCCTCTCGCAAGGACGGTC; RP, 5′-GTGTGTGCGTGGCTTCACTC; CXCL10 (280 bp): FP, 5′-GCTCCTGCATCAGCACCAGC; RP, 5′-CTTGAACGACGACGACTTTGG.

Fluorescence Cell Labeling and Imaging

Tag-Th1 cells (10^6) were labeled with 5 μl Cy5 fluorescent dye (Vibrant DiD cell labeling solution, Molecular Probes, Leiden, The Netherlands). Whole organ fluorescence of the pancreas and lymph nodes was imaged using a cooled ORCA-II-ER coupled charged device (CCD) camera (Hamamatsu, Hamamatsu, Japan). Bright-field images were performed with a photo camera (AE1, Canon, Krefeld, Germany). For quantitative fluorescence analysis, pancreata, lymph nodes, liver, and spleen were frozen in OCT compound (Tissue Tek, Vogel, Germany), and 20 μm cryostat sections were analyzed using a Storm Phosphor Imager (Amersham Bioscience, Sunnyvale, CA) in fluorescence mode. Quantitative analysis (focus to background ratio) of infiltrating Cy5-labeled Tag-Th1 cells was performed with ImageQuant 5.1 software (Amersham Bioscience) by comparing regions of interest in normal pancreatic tissue with regions of the same size with highest uptake.

Phosphor Storage Autoradiography

Three hours after i.v. injection of 370 kBq [^{125}I]Gluco-RGD, animals were sacrificed and tissue was isolated. Autoradiograms of the pancreas (20 μm fresh frozen sections) were obtained using a PhosphorImager 445SI (Amersham Bioscience). Quantitative analysis of [^{125}I]Gluco-RGD uptake (focus to background ratio) was performed with ImageQuant 5.1 software as described above.

Statistical Analysis

For statistical analysis of blood glucose levels in different groups, the mean value for each group and week was used to calculate linear regression curves. The respective slopes were then compared by t testing. In all groups, the variation of the two blood glucose measurements per mouse in the same week

was below 10% of the blood glucose level at the start of the experiment. Statistical analysis of survival and autoradiography data was performed with the Mann-Whitney-Wilcoxon test. Statistical analysis of tumor burden, tumor frequency, and tumor vessel density was performed with the Student's t test. $p < 0.05$ was considered statistically significant.

SUPPLEMENTAL DATA

The Supplemental Data include seven supplemental figures and can be found with this article online at http://www.cancercell.org/cgi/content/full/13/6/507/DC1/.

ACKNOWLEDGMENTS

We thank Drs. H. Wagner and G. Riethmüller (Munich), H.-G. Rammensee (Tübingen), J.-C. Cerottini (Lausanne), and J. Folkman and K. Javaherian (Boston) for discussions and critical reading of the manuscript. We thank Dr. Bernhard Puppe for the statistical analysis. We appreciate the technical support of C. Bodenstein, D. Dick, S. Harrasser, S. Hegewald, C. Jakobec, D. Jakob, S. Moosmann, and C. Reitmeier. The work was supported by the Deutsche Forschungsgemeinschaft RO 764/8-3, SFB 456, SFB 685, Wilhelm Sander-Stiftung (2005.043.1), and Deutsche Krebshilfe (107128). This work is part of the doctoral thesis of N.M.-H. and K.S.

Received: April 20, 2004
Revised: May 23, 2007
Accepted: April 8, 2008
Published: June 9, 2008

REFERENCES

Abbas, A.K., Murphy, K.M., and Sher, A. (1996). Functional diversity of helper T lymphocytes. Nature *383*, 787–793.

Agrawal, S., Agarwal, M.L., Chatterjee-Kishore, M., Stark, G.R., and Chisolm, G.M. (2002). Stat1-dependent, p53-independent expression of p21(waf1) modulates oxysterol-induced apoptosis. Mol. Cell. Biol. *22*, 1981–1992.

Arnott, C.H., Scott, K.A., Moore, R.J., Robinson, S.C., Thompson, R.G., and Balkwill, F.R. (2004). Expression of both TNF-alpha receptor subtypes is essential for optimal skin tumour development. Oncogene *23*, 1902–1910.

Baluk, P., Morikawa, S., Haskell, A., Mancuso, M., and McDonald, D.M. (2003). Abnormalities of basement membrane on blood vessels and endothelial sprouts in tumors. Am. J. Pathol. *163*, 1801–1815.

Bergers, G., Javaherian, K., Lo, K.M., Folkman, J., and Hanahan, D. (1999). Effects of angiogenesis inhibitors on multistage carcinogenesis in mice. Science *284*, 808–812.

Bergers, G., Brekken, R., McMahon, G., Vu, T.H., Itoh, T., Tamaki, K., Tanzawa, K., Thorpe, P., Itohara, S., Werb, Z., and Hanahan, D. (2000). Matrix metalloproteinase-9 triggers the angiogenic switch during carcinogenesis. Nat. Cell Biol. *2*, 737–744.

Berner, V., Liu, H., Zhou, Q., Alderson, K.L., Sun, K., Weiss, J.M., Back, T.C., Longo, D.L., Blazar, B.R., Wiltrout, R.H., et al. (2007). IFN-gamma mediates CD4(+) T-cell loss and impairs secondary antitumor responses after successful initial immunotherapy. Nat. Med. *13*, 354–360.

Bhowmick, N.A., Neilson, E.G., and Moses, H.L. (2004). Stromal fibroblasts in cancer initiation and progression. Nature *432*, 332–337.

Biedermann, T., Zimmermann, S., Himmelrich, H., Gumy, A., Egeter, O., Sakrauski, A.K., Seegmuller, I., Voigt, H., Launois, P., Levine, A.D., et al. (2001). IL-4 instructs TH1 responses and resistance to Leishmania major in susceptible BALB/c mice. Nat. Immunol. *2*, 1054–1060.

Billiau, A. (1996). Interferon-gamma: Biology and role in pathogenesis. Adv. Immunol. *62*, 61–130.

Bissell, M.J., and Radisky, D. (2001). Putting tumours in context. Nat. Rev. Cancer *1*, 46–54.

Boehm, U., Klamp, T., Groot, M., and Howard, J.C. (1997). Cellular responses to interferon-gamma. Annu. Rev. Immunol. *15*, 749–795.

Boon, T., Coulie, P.G., Van den Eynde, B.J., and van der Bruggen, P. (2006). Human T cell responses against melanoma. Annu. Rev. Immunol. *24*, 175–208.

Carmeliet, P., and Jain, R.K. (2000). Angiogenesis in cancer and other diseases. Nature *407*, 249–257.

Carswell, E.A., Old, L.J., Kassel, R.L., Green, S., Fiore, N., and Williamson, B. (1975). An endotoxin-induced serum factor that causes necrosis of tumors. Proc. Natl. Acad. Sci. USA *72*, 3666–3670.

Casanovas, O., Hager, J.H., Chun, M.G., and Hanahan, D. (2005a). Incomplete inhibition of the Rb tumor suppressor pathway in the context of inactivated p53 is sufficient for pancreatic islet tumorigenesis. Oncogene *24*, 6597–6604.

Casanovas, O., Hicklin, D.J., Bergers, G., and Hanahan, D. (2005b). Drug resistance by evasion of antiangiogenic targeting of VEGF signaling in late-stage pancreatic islet tumors. Cancer Cell *8*, 299–309.

Chamoto, K., Wakita, D., Narita, Y., Zhang, Y., Noguchi, D., Ohnishi, H., Iguchi, T., Sakai, T., Ikeda, H., and Nishimura, T. (2006). An essential role of antigen-presenting cell/T-helper type 1 cell-cell interactions in draining lymph node during complete eradication of class II-negative tumor tissue by T-helper type 1 cell therapy. Cancer Res. *66*, 1809–1817.

Daniel, D., Meyer-Morse, N., Bergsland, E.K., Dehne, K., Coussens, L.M., and Hanahan, D. (2003). Immune enhancement of skin carcinogenesis by CD4+ T cells. J. Exp. Med. *197*, 1017–1028.

Daniel, D., Chiu, C., Giraudo, E., Inoue, M., Mizzen, L.A., Chu, N.R., and Hanahan, D. (2005). CD4+ T cell-mediated antigen-specific immunotherapy in a mouse model of cervical cancer. Cancer Res. *65*, 2018–2025.

de Visser, K.E., Eichten, A., and Coussens, L.M. (2006). Paradoxical roles of the immune system during cancer development. Nat. Rev. Cancer *6*, 24–37.

Egeter, O., Mocikat, R., Ghoreschi, K., Dieckmann, A., and Rocken, M. (2000). Eradication of disseminated lymphomas with CpG-DNA activated T helper type 1 cells from nontransgenic mice. Cancer Res. *60*, 1515–1520.

Folkman, J., Watson, K., Ingber, D., and Hanahan, D. (1989). Induction of angiogenesis during the transition from hyperplasia to neoplasia. Nature *339*, 58–61.

Forster, I., Hirose, R., Arbeit, J.M., Clausen, B.E., and Hanahan, D. (1995). Limited capacity for tolerization of CD4+ T cells specific for a pancreatic beta cell neo-antigen. Immunity *2*, 573–585.

Ganss, R., Ryschich, E., Klar, E., Arnold, B., and Hammerling, G.J. (2002). Combination of T-cell therapy and trigger of inflammation induces remodeling of the vasculature and tumor eradication. Cancer Res. *62*, 1462–1470.

Garbi, N., Arnold, B., Gordon, S., Hammerling, G.J., and Ganss, R. (2004). CpG motifs as proinflammatory factors render autochthonous tumors permissive for infiltration and destruction. J. Immunol. *172*, 5861–5869.

Garcia-Lora, A., Algarra, I., and Garrido, F. (2003). MHC class I antigens, immune surveillance, and tumor immune escape. J. Cell. Physiol. *195*, 346–355.

Greenberg, P.D. (1991). Adoptive T cell therapy of tumors: Mechanisms operative in the recognition and elimination of tumor cells. Adv. Immunol. *49*, 281–355.

Haagsma, E.B., Hagens, V.E., Schaapveld, M., van den Berg, A.P., de Vries, E.G., Klompmaker, I.J., Slooff, M.J., and Jansen, P.L. (2001). Increased cancer risk after liver transplantation: A population-based study. J. Hepatol. *34*, 84–91.

Hanahan, D., and Weinberg, R.A. (2000). The hallmarks of cancer. Cell *100*, 57–70.

Haubner, R., Wester, H.J., Weber, W.A., Mang, C., Ziegler, S.I., Goodman, S.L., Senekowitsch-Schmidtke, R., Kessler, H., and Schwaiger, M. (2001). Noninvasive imaging of alpha(v)beta3 integrin expression using 18F-labeled RGD-containing glycopeptide and positron emission tomography. Cancer Res. *61*, 1781–1785.

Holmgren, L., Ambrosino, E., Birot, O., Tullus, C., Veitonmaki, N., Levchenko, T., Carlson, L.M., Musiani, P., Iezzi, M., Curcio, C., et al. (2006). A DNA vaccine targeting angiomotin inhibits angiogenesis and suppresses tumor growth. Proc. Natl. Acad. Sci. USA *103*, 9208–9213.

Indraccolo, S., Pfeffer, U., Minuzzo, S., Esposito, G., Roni, V., Mandruzzato, S., Ferrari, N., Anfosso, L., Dell'Eva, R., Noonan, D.M., et al. (2007). Identification

of genes selectively regulated by IFNs in endothelial cells. J. Immunol. *178*, 1122–1135.

Inoue, M., Hager, J.H., Ferrara, N., Gerber, H.P., and Hanahan, D. (2002). VEGF-A has a critical, nonredundant role in angiogenic switching and pancreatic beta cell carcinogenesis. Cancer Cell *1*, 193–202.

Kaplan, D.H., Shankaran, V., Dighe, A.S., Stockert, E., Aguet, M., Old, L.J., and Schreiber, R.D. (1998). Demonstration of an interferon gamma-dependent tumor surveillance system in immunocompetent mice. Proc. Natl. Acad. Sci. USA *95*, 7556–7561.

Koebel, C.M., Vermi, W., Swann, J.B., Zerafa, N., Rodig, S.J., Old, L.J., Smyth, M.J., and Schreiber, R.D. (2007). Adaptive immunity maintains occult cancer in an equilibrium state. Nature *450*, 903–907.

Lin, E.Y., Nguyen, A.V., Russell, R.G., and Pollard, J.W. (2001). Colony-stimulating factor 1 promotes progression of mammary tumors to malignancy. J. Exp. Med. *193*, 727–740.

Lin, W.W., and Karin, M. (2007). A cytokine-mediated link between innate immunity, inflammation, and cancer. J. Clin. Invest. *117*, 1175–1183.

MacKie, R.M., Reid, R., and Junor, B. (2003). Fatal melanoma transferred in a donated kidney 16 years after melanoma surgery. N. Engl. J. Med. *348*, 567–568.

Mocikat, R., Braumuller, H., Gumy, A., Egeter, O., Ziegler, H., Reusch, U., Bubeck, A., Louis, J., Mailhammer, R., Riethmuller, G., et al. (2003). Natural killer cells activated by MHC class I(low) targets prime dendritic cells to induce protective CD8 T cell responses. Immunity *19*, 561–569.

Moore, R.J., Owens, D.M., Stamp, G., Arnott, C., Burke, F., East, N., Holdsworth, H., Turner, L., Rollins, B., Pasparakis, M., et al. (1999). Mice deficient in tumor necrosis factor-alpha are resistant to skin carcinogenesis. Nat. Med. *5*, 828–831.

Mumberg, D., Monach, P.A., Wanderling, S., Philip, M., Toledano, A.Y., Schreiber, R.D., and Schreiber, H. (1999). CD4(+) T cells eliminate MHC class II-negative cancer cells in vivo by indirect effects of IFN-gamma. Proc. Natl. Acad. Sci. USA *96*, 8633–8638.

Nanni, P., Nicoletti, G., De Giovanni, C., Landuzzi, L., Di Carlo, E., Cavallo, F., Pupa, S.M., Rossi, I., Colombo, M.P., Ricci, C., et al. (2001). Combined allogeneic tumor cell vaccination and systemic interleukin 12 prevents mammary carcinogenesis in HER-2/neu transgenic mice. J. Exp. Med. *194*, 1195–1205.

Nelson, D.J., Mukherjee, S., Bundell, C., Fisher, S., van Hagen, D., and Robinson, B. (2001). Tumor progression despite efficient tumor antigen cross-presentation and effective "arming" of tumor antigen-specific CTL. J. Immunol. *166*, 5557–5566.

Nishikawa, H., Kato, T., Tawara, I., Ikeda, H., Kuribayashi, K., Allen, P.M., Schreiber, R.D., Old, L.J., and Shiku, H. (2005). IFN-gamma controls the generation/activation of CD4+ CD25+ regulatory T cells in antitumor immune response. J. Immunol. *175*, 4433–4440.

Nozawa, H., Chiu, C., and Hanahan, D. (2006). Infiltrating neutrophils mediate the initial angiogenic switch in a mouse model of multistage carcinogenesis. Proc. Natl. Acad. Sci. USA *103*, 12493–12498.

Olieman, A.F., Lienard, D., Eggermont, A.M., Kroon, B.B., Lejeune, F.J., Hoekstra, H.J., and Koops, H.S. (1999). Hyperthermic isolated limb perfusion with tumor necrosis factor alpha, interferon gamma, and melphalan for locally advanced nonmelanoma skin tumors of the extremities: A multicenter study. Arch. Surg. *134*, 303–307.

Otahal, P., Schell, T.D., Hutchinson, S.C., Knowles, B.B., and Tevethia, S.S. (2006). Early immunization induces persistent tumor-infiltrating CD8+ T cells against an immunodominant epitope and promotes lifelong control of pancreatic tumor progression in SV40 tumor antigen transgenic mice. J. Immunol. *177*, 3089–3099.

Pannellini, T., Spadaro, M., Di Carlo, E., Ambrosino, E., Iezzi, M., Amici, A., Lollini, P.L., Forni, G., Cavallo, F., and Musiani, P. (2006). Timely DNA vaccine combined with systemic IL-12 prevents parotid carcinomas before a dominant-negative p53 makes their growth independent of HER-2/neu expression. J. Immunol. *176*, 7695–7703.

Pfaff, M., Tangemann, K., Muller, B., Gurrath, M., Muller, G., Kessler, H., Timpl, R., and Engel, J. (1994). Selective recognition of cyclic RGD peptides of NMR defined conformation by alpha IIb beta 3, alpha V beta 3, and alpha 5 beta 1 integrins. J. Biol. Chem. *269*, 20233–20238.

Pfeffer, K., Matsuyama, T., Kundig, T.M., Wakeham, A., Kishihara, K., Shahinian, A., Wiegmann, K., Ohashi, P.S., Kronke, M., and Mak, T.W. (1993). Mice deficient for the 55 kd tumor necrosis factor receptor are resistant to endotoxic shock, yet succumb to L. monocytogenes infection. Cell *73*, 457–467.

Prehn, R.T. (1972). The immune reaction as a stimulator of tumor growth. Science *176*, 170–171.

Qin, Z., and Blankenstein, T. (2000). CD4+ T cell-mediated tumor rejection involves inhibition of angiogenesis that is dependent on IFN gamma receptor expression by nonhematopoietic cells. Immunity *12*, 677–686.

Racke, M.K., Bonomo, A., Scott, D.E., Cannella, B., Levine, A., Raine, C.S., Shevach, E.M., and Rocken, M. (1994). Cytokine-induced immune deviation as a therapy for inflammatory autoimmune disease. J. Exp. Med. *180*, 1961–1966.

Ramana, C.V., Grammatikakis, N., Chernov, M., Nguyen, H., Goh, K.C., Williams, B.R., and Stark, G.R. (2000). Regulation of c-myc expression by IFN-gamma through Stat1-dependent and -independent pathways. EMBO J. *19*, 263–272.

Rosenberg, S.A., Yang, J.C., and Restifo, N.P. (2004). Cancer immunotherapy: Moving beyond current vaccines. Nat. Med. *10*, 909–915.

Ruegg, C., Yilmaz, A., Bieler, G., Bamat, J., Chaubert, P., and Lejeune, F.J. (1998). Evidence for the involvement of endothelial cell integrin alphaVbeta3 in the disruption of the tumor vasculature induced by TNF and IFN-gamma. Nat. Med. *4*, 408–414.

Sato, E., Olson, S.H., Ahn, J., Bundy, B., Nishikawa, H., Qian, F., Jungbluth, A.A., Frosina, D., Gnjatic, S., Ambrosone, C., et al. (2005). Intraepithelial CD8+ tumor-infiltrating lymphocytes and a high CD8+/regulatory T cell ratio are associated with favorable prognosis in ovarian cancer. Proc. Natl. Acad. Sci. USA *102*, 18538–18543.

Schadendorf, D., Ugurel, S., Schuler-Thurner, B., Nestle, F.O., Enk, A., Brocker, E.B., Grabbe, S., Rittgen, W., Edler, L., Sucker, A., et al. (2006). Dacarbazine (DTIC) versus vaccination with autologous peptide-pulsed dendritic cells (DC) in first-line treatment of patients with metastatic melanoma: A randomized phase III trial of the DC study group of the DeCOG. Ann. Oncol. *17*, 563–570.

Schultz, E.S., Schuler-Thurner, B., Stroobant, V., Jenne, L., Berger, T.G., Thielemanns, K., van der Bruggen, P., and Schuler, G. (2004). Functional analysis of tumor-specific Th cell responses detected in melanoma patients after dendritic cell-based immunotherapy. J. Immunol. *172*, 1304–1310.

Shankaran, V., Ikeda, H., Bruce, A.T., White, J.M., Swanson, P.E., Old, L.J., and Schreiber, R.D. (2001). IFNgamma and lymphocytes prevent primary tumour development and shape tumour immunogenicity. Nature *410*, 1107–1111.

Siegel, C.T., Schreiber, K., Meredith, S.C., Beck-Engeser, G.B., Lancki, D.W., Lazarski, C.A., Fu, Y.X., Rowley, D.A., and Schreiber, H. (2000). Enhanced growth of primary tumors in cancer-prone mice after immunization against the mutant region of an inherited oncoprotein. J. Exp. Med. *191*, 1945–1956.

Soucek, L., Lawlor, E.R., Soto, D., Shchors, K., Swigart, L.B., and Evan, G.I. (2007). Mast cells are required for angiogenesis and macroscopic expansion of Myc-induced pancreatic islet tumors. Nat. Med. *13*, 1211–1218.

Speiser, D.E., Miranda, R., Zakarian, A., Bachmann, M.F., McKall-Faienza, K., Odermatt, B., Hanahan, D., Zinkernagel, R.M., and Ohashi, P.S. (1997). Self antigens expressed by solid tumors do not efficiently stimulate naive or activated T cells: Implications for immunotherapy. J. Exp. Med. *186*, 645–653.

Spiotto, M.T., Rowley, D.A., and Schreiber, H. (2004). Bystander elimination of antigen loss variants in established tumors. Nat. Med. *10*, 294–298.

Stewart, T., Tsai, S.C., Grayson, H., Henderson, R., and Opelz, G. (1995). Incidence of de-novo breast cancer in women chronically immunosuppressed after organ transplantation. Lancet *346*, 796–798.

Stoelcker, B., Ruhland, B., Hehlgans, T., Bluethmann, H., Luther, T., and Mannel, D.N. (2000). Tumor necrosis factor induces tumor necrosis via tumor necrosis factor receptor type 1-expressing endothelial cells of the tumor vasculature. Am. J. Pathol. *156*, 1171–1176.

Street, S.E., Trapani, J.A., MacGregor, D., and Smyth, M.J. (2002). Suppression of lymphoma and epithelial malignancies effected by interferon gamma. J. Exp. Med. *196*, 129–134.

Suganuma, M., Okabe, S., Marino, M.W., Sakai, A., Sueoka, E., and Fujiki, H. (1999). Essential role of tumor necrosis factor alpha (TNF-alpha) in tumor promotion as revealed by TNF-alpha-deficient mice. Cancer Res. *59*, 4516–4518.

Suganuma, M., Kuzuhara, T., Yamaguchi, K., and Fujiki, H. (2006). Carcinogenic role of tumor necrosis factor-alpha inducing protein of Helicobacter pylori in human stomach. J. Biochem. Mol. Biol. *39*, 1–8.

Tannenbaum, C.S., Tubbs, R., Armstrong, D., Finke, J.H., Bukowski, R.M., and Hamilton, T.A. (1998). The CXC chemokines IP-10 and Mig are necessary for IL-12-mediated regression of the mouse RENCA tumor. J. Immunol. *161*, 927–932.

Valmori, D., Dutoit, V., Rubio-Godoy, V., Chambaz, C., Lienard, D., Guillaume, P., Romero, P., Cerottini, J.C., and Rimoldi, D. (2001). Frequent cytolytic T-cell responses to peptide MAGE-A10(254–262) in melanoma. Cancer Res. *61*, 509–512.

Willimsky, G., and Blankenstein, T. (2005). Sporadic immunogenic tumours avoid destruction by inducing T-cell tolerance. Nature *437*, 141–146.

Yao, V.J., Ozawa, M.G., Varner, A.S., Kasman, I.M., Chanthery, Y.H., Pasqualini, R., Arap, W., and McDonald, D.M. (2006). Antiangiogenic therapy decreases integrin expression in normalized tumor blood vessels. Cancer Res. *66*, 2639–2649.

Yee, C., Thompson, J.A., Byrd, D., Riddell, S.R., Roche, P., Celis, E., and Greenberg, P.D. (2002). Adoptive T cell therapy using antigen-specific CD8+ T cell clones for the treatment of patients with metastatic melanoma: In vivo persistence, migration, and antitumor effect of transferred T cells. Proc. Natl. Acad. Sci. USA *99*, 16168–16173.

Zitvogel, L. (2002). Dendritic and natural killer cells cooperate in the control/switch of innate immunity. J. Exp. Med. *195*, F9–F14.